Heliyon

Received:
14 January 2018
Revised:
30 May 2018
Accepted:
11 September 2018

Cite as: Hamid Aziz, Aamer Saeed, Farukh Jabeen, Noor ud Din, Ulrich Flörke. Synthesis, single crystal analysis, biological and docking evaluation of tetrazole derivatives. Heliyon 4 (2018) e00792. doi: 10.1016/j.heliyon.2018.e00792

Synthesis, single crystal analysis, biological and docking evaluation of tetrazole derivatives

Hamid Aziz [a], **Aamer Saeed** [a,*], **Farukh Jabeen** [b], **Noor ud Din** [a], **Ulrich Flörke** [c]

[a] *Department of Chemistry, Quaid-I-Azam University Islamabad, 45320 Pakistan*

[b] *Cardiovascular and Metabolic Research Unit, Laurentian University, 935 Ramsey Lake Road, Sudbury, ON, P3E 2C6, Canada*

[c] *Department Chemie, Fakultätfür Naturwissenschaften, Universität Paderborn, Warburgerstraße 100, 33098 Paderborn, Germany*

[*] Corresponding author.

E-mail addresses: aamersaeed@yahoo.com, asaeed@qau.edu.pk (A. Saeed).

Abstract

Tetrazoles are conjugated nitrogen-rich heterocycles considered as bio-isosteres of carboxylic acids. Tetrazoles owing to their conjugated structures serve as biologically relevant potent scaffolds. The present research paper reports the successful synthesis and single crystal analysis of three different tetrazole derivatives **(2, 4, 6)**. The synthesized tetrazole derivatives were evaluated for their possible cytotoxicity LD_{50} (52.89, 49.33, 17.28 μg/ml) and antileishmanial activities IC_{50} (0.166, 10, 5.0 μg/ml). Moreover, molecular docking studies were performed to determine the possible interaction sites of the tetrazole derivatives **(2, 4, 6)** with TryR, an enzyme involved in the redox metabolism of the *Leishmania* parasite. Docking computations demonstrates that the tetrazole derivatives **(2, 4, 6)** established prominent binding interactions with the key residues of the TryR and possess the potential to effectively inhibit the catalytic activities of the enzyme. The results suggested that the synthesized tetrazole derivative **(2, 4, 6)** can be possible hit candidates which can be tested further against amastigote stage of parasite and then in an animal model of leishmaniasis.

https://doi.org/10.1016/j.heliyon.2018.e00792

Keywords: Biochemistry, Pharmaceutical chemistry, Organic chemistry

1. Introduction

Tetrazoles are Nitrogen-rich five-member heterocycles having carbon and four nitrogen atoms arranged in a planar ring [1, 2]. Tetrazoles serve as non-classical isosteres of carboxylic acids owing to their close pK_a values, physiological pH and a maximum nitrogen content of any heterocycles. The nitrogen-rich conjugated system confers tetrazoles with both donor and acceptor electronic properties [3]. The planar structure stabilizes negative charge by delocalization which is considered favorable for the receptor-ligand interaction. Tetrazolate anions are more lipophilic than carboxylates, which benefits the passage of drug molecules through cell membranes. Furthermore, tetrazoles are resistant to metabolic degradation pathways thus possess a longer duration of action [4].

Tetrazoles and their heterocyclic analogues are termed as important pharmacophores in medicinal chemistry owing to their unique structure and favorable pharmacokinetic profile. Their pharmacological profile includes antihypertensive, anti-analgesic, anti-ulcer and anti-allergic activities [5, 6, 7, 8, 9]. Tetrazoles based heterocycles have wide synthetic utility and serve as a precursor for the synthesis of potent heterocycles including propellants, explosives and pharmaceuticals [10, 11]. Heterocyclic analogues of tetrazoles serve as the first approved treatment for the partial agonist of dopamine D2 receptors [12, 13]. Tetrazoles based heterocycles serve as potent anticancer and antimicrobial agents [14]. Jack man *et al.* reports the potent cytotoxicity and growth inhibitory activities of tetrazoles containing drugs. Tetrazoles based drugs have incomplete overlapping spectrum of antitumor activity and toxicity profile compared with tomudex and possibly other Thymidylate synthase inhibitors currently being studied clinically [15]. Leishmaniasis is a zoonosis that is transmitted between vertebrates and humans through sandfly. Literature survey reveals tetrazoles based heterocycles as potent antileishmanial agents. In this context, Pyrazolyl based tetrazoles are reported to be effective antileishmanial and cytotoxicity agents [16]. Similarly Faiões *et al.* reports the synthesis, antileishmanial potential and oral bioavailability of 5-[5-amino-1-(4′-methoxyphenyl)1*H*-pyrazole-4-yl]1*H*-tetrazole using a rational drug design approach [17]. Recently Viviane *et al.* reported the antileishmanial potential of arylpyrazole based tetrazoles. The synthesized arylpyrazole based tetrazoles displayed potent and innovative antileishmanial response [18].

Thus keeping in view the exciting pharmacological profile of tetrazoles and their heterocyclic analogues, herein we report the facile synthesis and characterization of three differently substituted tetrazole derivatives **(2, 4, 6)** from commercially available substituted aromatic amines using sodium azide and triethyl orthoformate. The

https://doi.org/10.1016/j.heliyon.2018.e00792

synthesis proceeds at reflux temperatures in the presence of glacial acetic acid. Upon successful completion of the reaction, crystals of the synthesized tetrazole derivatives **(2, 4, 6)** were grown from their supersaturated solutions and were characterized using single crystal XRD. The synthesized tetrazole derivatives **(2, 4, 6)** were tested for their cytotoxic and antileishmanial potential. Computational molecular docking studies were carried out to study the binding mode of the synthesized tetrazole derivatives **(2, 4, 6)**.

2. Results and discussion

2.1. Synthesis of (2, 4, 6)

Tetrazoles are nitrogen-rich heterocycles which display wide and potent spectrum of biological activities. The best known method for the synthesis of Tetrazoles is by treating sodium azide and triethyl orthoformate with aromatic amines in glacial acetic acid as shown in Fig. 1 [19]. Using this synthetic methodology, three different tetrazole derivatives **(2, 4, 6)** were successfully synthesized in higher yields. However, to the best of our knowledge, the synthesized tetrazole derivatives **(4, 6)** were found to be reported by Alexender *et al.* and Zhao *et al* respectively as clearly evident from the reference [20, 21].

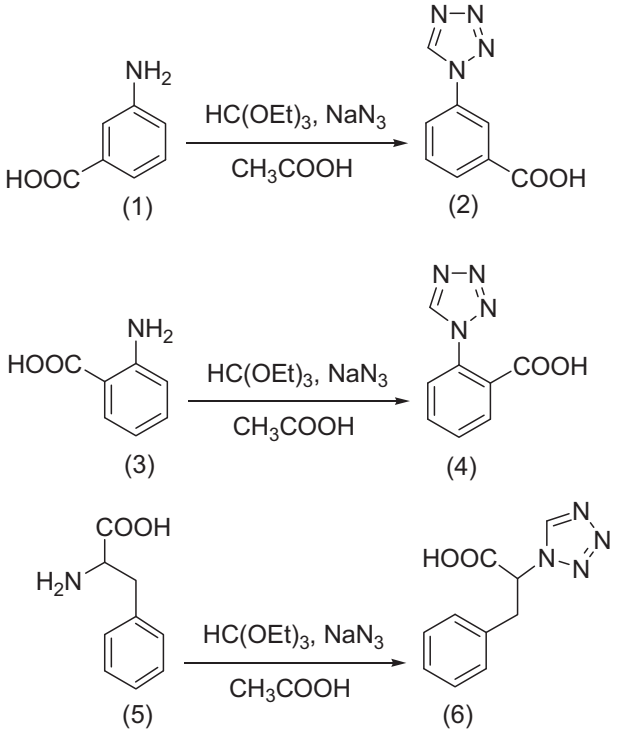

Fig. 1. Synthesis of the different tetrazole derivatives **(2, 4, 6)**.

https://doi.org/10.1016/j.heliyon.2018.e00792

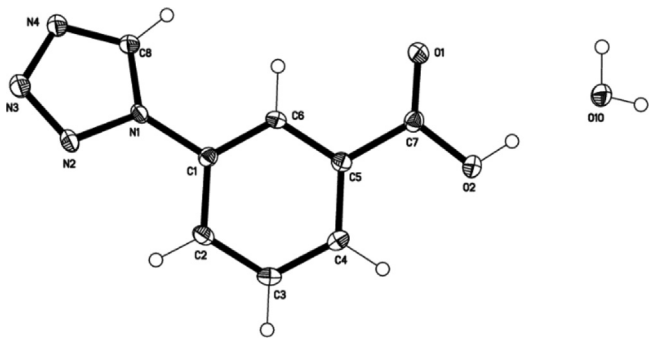

Fig. 2. Molecular structure of **(2)** · $\mathbf{H_2O}$. Anisotropic displacement ellipsoids are drawn at the 50% probability level.

2.2. X-ray crystal structure description for the synthesized tetrazole derivatives (2, 4, 6)

2.2.1. X-ray crystal structure description for the tetrazole derivative (2)·H_2O

The molecular structure of **(2)** (Fig. 2) is related to that of 2-(1*H*-tetrazol-1-yl)benzoic acid [21]. **(2)** shows the benzoic acid moiety co-planar with the aromatic ring plane, the relevant torsion angle is O2-C7-C5-C40.01(19)°, but the tetrazole ring is twisted relative to the C_6 ring plane, the torsion angle N2-N1-C1-C2 measures 25.95(19)°. Other relevant geometries are N1-N2 1.3549(16), N2-N3 1.2930(16), N3-N4 1.3582(16), N4-C8 1.3122(18), N1-C8 1.3395(16), N1-C1 1.4341(16).

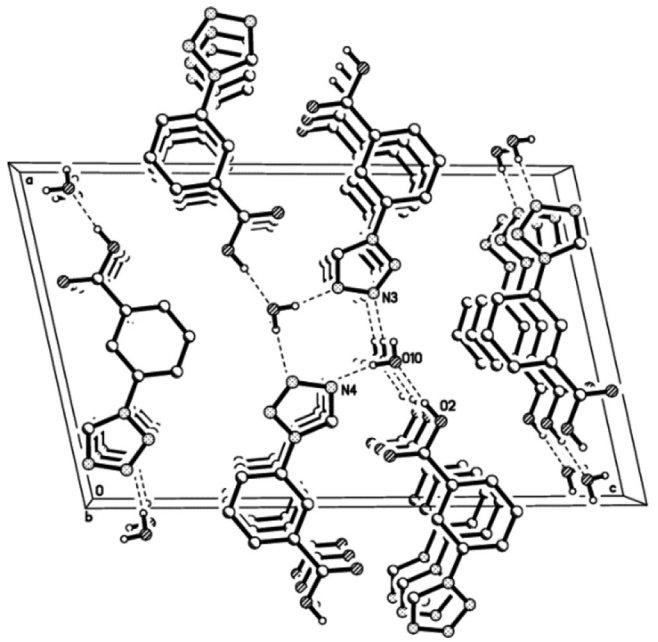

Fig. 3. Unit cell with intermolecular H-bonding pattern as dotted lines, viewed along *b*-axis. H atoms not involved are omitted.

https://doi.org/10.1016/j.heliyon.2018.e00792

The crystal packing (Fig. 3) shows short hydrogen bonds between the water solvent molecule and **(2)**: O2-H…O10 with H…O 1.759 Å and O-H…O 172.7°; O10-H11…N3*(x + 1, y − 1, z)* with H…N 2.071 Å and O-H…N 172.4°; O10-H12…N4*(−x + 1, −y + 1, −z)* with H…N 2.054 Å and O-H…N 167.8°. These interactions connect molecules into endless double chains that extend along [100]. Crystal data and structure refinement for **(2)** is provided in Table 1.

2.2.2. X-ray crystal structure description for the tetrazole derivatives (2, 6)

Molecular structures of tetrazole derivatives **(4, 6)** are given below in Figs. 3 and 4 respectively. The single crystal XRD analysis data of the tetrazole derivatives **(2, 4)**

Table 1. Crystal data and structure refinement for **(2)**.

Empirical formula	C_8 H_8 N_4 O_3
Formula weight	208.18
T (K)	130(2) K
Wavelength	0.71073 Å
Crystal system	Monoclinic
Space group	P2(1)/n
Unit cell dimensions	
a = 12.435(2) Å	α = 90°.
b = 3.6715(6) Å	β = 102.511(4)°.
c = 20.015(3) Å	δ = 90°.
V (Å$^{3)}$	763.547(15)
Z	4
Density (calculated)	1.550 Mg/m^3
Absorption co-efficient	0.122 mm^{-1}
F(000)	432
Crystal size	0.46 × 0.08 × 0.06 mm^3
Theta range for data collection	1.77 to 27.88°.
Reflections collected	7739
Independent reflections	2109 [R(int) = 0.0326]
Completeness to theta = 27.88°	99.7 %
Absorption correction	Semi-empirical from equivalents
Max. and min. transmission	0.9927 and 0.9459
Refinement method	Full-matrix least-squares on F^2
Data/restraints/parameters	2109/3/145
Goodness-of-fit on F^2	1.036
Final R indices [I > 2sigma(I)]	R1 = 0.0388, wR2 = 0.0995
R indices (all data)	R1 = 0.0499, wR2 = 0.1072
Largest diff. peak and hole	0.350 and −0.212 e.Å^{-3}

https://doi.org/10.1016/j.heliyon.2018.e00792

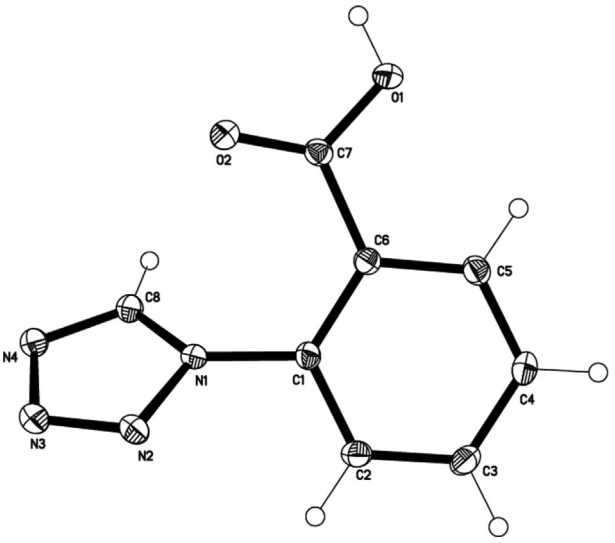

Fig. 4. Single crystal XRD analyzed molecular structure of **(4)**.

is presented in Tables 2 and 3 respectively. The tetrazole derivatives **(2, 4)** are reported as mentioned in references [20, 21] (see Fig. 5).

2.3. Biological activities of the synthesized tetrazole derivatives (2, 4, 6)

In vitro cytotoxicity and antileishmanial activities were performed in favor of the synthesized tetrazole derivatives **(2, 4, 6)**. Human red blood cells (Human red blood cells, approved by the review committee of the Biotechnology Department, Quaid-i-Azam University, Islamabad, Pakistan, on February 7, 2014; the subjects also provided informed consent) were selected to perform cytotoxicity of the synthesized tetrazole derivative **(2, 4, 6)**. The release of hemoglobin from red blood cells determined the cytotoxicity of **(2, 4, 6)**, measured using Uv-visible spectroscopy. The extent of hemolysis was compared to that produced by Triton X-100 as a control and was found to be significantly less for the tested tetrazole derivatives **(2, 4, 6)**. The cytotoxicity data in terms of their LD_{50} values is given below in Table 4. Based on this data, it was found that the tested tetrazole derivatives **(2, 4, 6)** are biocompatible.

The ability of tetrazole derivatives **(2, 4, 6)** to act an antileishmanial agents against the promastigotes of *Leishmania tropica* was assayed using Glucantime as a positive and DMSO as a negative control. Glucantime is a drug used in treatment of cutaneous leishmaniasis. The antileishmanial data in terms of their IC_{50} values are given below in Table 4. The results reveal that the tested tetrazole derivatives **(2, 4, 6)** act as an inhibitor of this genus of trypanosomes. It was shown to have maximum antileishmanial activity compared to an IC_{50} value of 7.44 μg/ml for the standard drug (Glucantime) [22].

https://doi.org/10.1016/j.heliyon.2018.e00792

Table 2. Crystal data and structure refinement for **(4)**.

Empirical formula	$C_8\ H_6\ N_4\ O_2$
Formula weight	190.16
T (K)	130(2) K
Wavelength	0.71073 Å
Crystal system	Monoclinic
Space group	P2(1)/n
Unit cell dimensions	
a = 3.7380(6) Å	α = 90°.
b = 16.030(3) Å	β = 90.785(3)°.
c = 13.250(2) Å	δ = 90°.
V (Å$^{3)}$	793.9(2) Å^3
Z	4
Density (calculated)	1.591 Mg/m^3
Absorption co-efficient	0.120 mm^{-1}
F(000)	392
Crystal size	0.300 × 0.260 × 0.160 mm^3
Theta range for data collection	1.994 to 27.875°
Index ranges	−4≤h≤4,−19≤k≤21, −17≤l≤17
Reflections collected	7362
Independent reflections	1877 [R(int) = 0.0212]
Completeness to theta = 27.88°	100.0 %
Absorption correction	Semi-empirical from equivalents
Max. and min. transmission	0.981 and 0.965
Refinement method	Full-matrix least-squares on F^2
Data/restraints/parameters	1877/0/128
Goodness-of-fit on F^2	1.044
Final R indices [I > 2sigma(I)]	R1 = 0.0347, wR2 = 0.0903
R indices (all data)	R1 = 0.0402, wR2 = 0.0945
Extinction coefficient	n/a
Largest diff. peak and hole	0.355 and −0.216 e.Å^{-3}

2.4. Molecular docking study

The tested tetrazole derivatives (**2, 4, 6**) were further investigated for their binding mode by performing molecular docking study. The result of the docking computation for the tetrazole derivative **(2, 4, 6)** are given below.

2.5. Results and discussion of docking computation of (2)

A theoretical docking study, for evaluation of ligand as an inhibitor of trypanothione reductase a validated drug target enzyme of the *Leishmania* parasite was conducted.

https://doi.org/10.1016/j.heliyon.2018.e00792

Table 3. Crystal data and structure refinement for (6).

Empirical formula	$C_{10}H_{12}N_4O_3$
Formula weight	236.24
T (K)	130(2) K
Wavelength	0.71073 Å
Crystal system	Orthorhombic
Space group	P2(1)2(1)2
Unit cell dimensions	
a = 23.972(3) Å	α = 90°.
b = 5.6823(7) Å	β = 90.
c = 8.2903(10) Å	δ = 90°.
V (Å$^{3)}$	1129.3(2) Å^3
Z	4
Density (calculated)	1.390 Mg/m^3
Absorption co-efficient	0.106 mm^{-1}
F(000)	496
Crystal size	0.40 × 0.28 × 0.22 mm^3
Theta range for data collection	1.70 to 27.88°.
Index ranges	−31≤h≤31, −7≤k≤7, −10≤l≤10
Reflections collected	10785
Independent reflections	1601 [R(int) = 0.0245]
Completeness to theta = 27.88°	100.0 %
Absorption correction	Semi-empirical from equivalents
Max. and min. transmission	0.9771 and 0.9589
Refinement method	Full-matrix least-squares on F^2
Data/restraints/parameters	1601/3/163
Goodness-of-fit on F^2	1.031
Final R indices [I > 2sigma(I)]	R1 = 0.0304, wR2 = 0.0815
R indices (all data)	R1 = 0.0330, wR2 = 0.0837
Absolute structure parameter	−1.3(12)
Largest diff. peak and hole	0.293 and −0.177 e.Å^{-3}

The enzyme trypanothione reductase (TryR) is involved in the redox metabolism of the leishmania parasite, and inhibition of TryR can potentially disturb the redox balance of the parasite leading to death of the parasite [23]. The synthesized tetrazole derivative **(2)** was computationally docked into the pocket of trypanothione reductase (TryR) enzyme, required for redox balance of the parasite. Glide docking module, offered by Schrodinger program was used to carry out the molecular docking of synthesized molecule on protein [24]. The compound under analysis showed satisfactory docking with acceptable statistics inside the active site of TryR. The enzyme (TryR) is a dimer and chain A was selected for the docking studies. Docking analysis

https://doi.org/10.1016/j.heliyon.2018.e00792

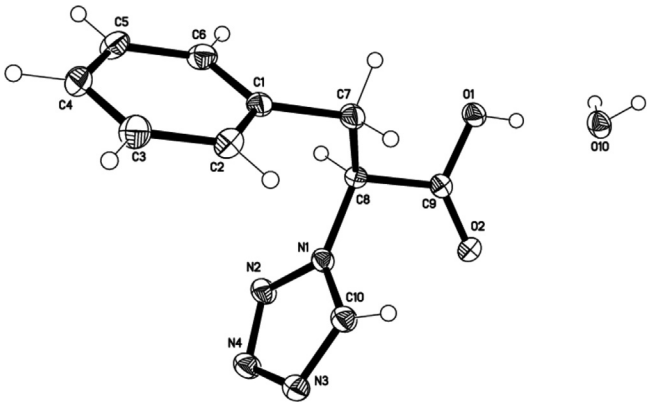

Fig. 5. Single crystal XRD analyzed molecular structure of **(6)**.

Table 4. Cytotoxicity and antileishmanial data of the tetrazole derivatives (2, 4, 6).

S. NO	Entry	Cytotoxicity LD_{50} (μg/ml)	Antileishmanial activity IC_{50} (μg/ml)	SI (LD_{50}/IC_{50})
1	2	52.89 ± 0.85	0.166 ± 0.032	318.6
2	4	49.33 ± 0.80	10 ± 0.1	4.93
3	6	17.28 ± 0.67	05 ± 0.053	3.456

of the ligand with TryR protein enabled us to identify specific residues which constructed the active site. Following residues, Lue10, Gly11, Ala12 Gly13, Ser14, Gly15, Gly16, Val34, Asp35, Val36, Ala46, Ala47, Gly49, Gly50, Thr51, Cys52, Gly125, Phe126, Gl127, Ala159, Thr160, Ser162, Arg290, Ala293, Leu294, Ile325, Gly326, Asp327, Val328, Ala338, Met333, Leu334, Thr335, and Ala338, are found surrounding docked poses of the ligand. These residues can possibly play an important functional roles in enzyme activities. Therefore, interaction of the ligand with these residues could influence the structure of the active site, consequently leading to inhibition of the activities of the enzyme TryR.

The detailed analysis of the binding mode of the ligand with TryR receptor revealed that the ligand stabilized itself inside the active site gorge through copious interactions with the atoms of the key residues of receptor.

Phenyl ring and tetrazole ring of the ligand formed π-π stacking with the phenyl ring of the Tyr198 as shown in Fig. 6a played a significant role in binding the molecule inside the active side. TryR. Ligand atoms stabilized itself through the copious strong hydrogen bonding with the amino acid residues inside the active site gorge of the TryR such as Asp327 O-H…O and Thr335 (O-H….O) as shown in Fig. 6b. In addition to that, a nitrogen atom of the tetrazole ring of the ligand established distinct hydrogen bonding (N-H….N) with Lys60 as shown in Fig. 6b. Fig. 7 represents the docked conformation of ligand inside the pockte of TyrR in two

https://doi.org/10.1016/j.heliyon.2018.e00792

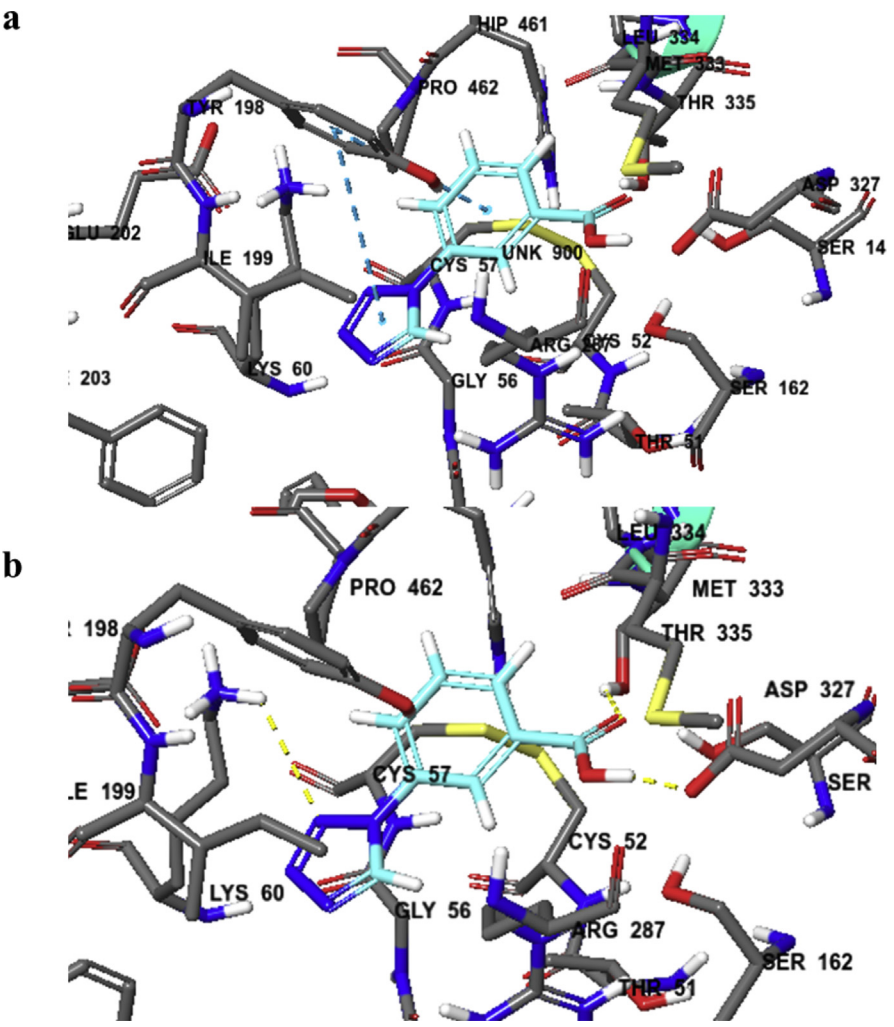

Fig. 6. Binding mode of tetrazole derivative **(2)** inside the active site of TryR. Docking poses of **(2)** in tri-dimensional space. Ligands is shown in ball and stick mode in elemental and cyan color and key residues are shown in stick mode, elemental color. a) π-π interaction of the aromatic ring of the ligand with the phenyl ring of Phe182 and Tyr198 is shown in cyan colored dashed lines. b) Hydrogen bonding of ligand atom with the amino acid residues is shown in pink colored dashed lines marked with distances.

dimensional space. Moreover, compound was found to interact favorably with TryR protein with a considerable docking and Glide score of −5. 29 kcal/mol.

2.6. Results and discussion of docking computation of (4)

In order to investigate the potential antileishmanial properties of the tetrazole derivative **(4)**, theoretical docking study was conducted on TryR and the compound. Trypanothione reductase (TryR) is involved in the redox metabolism of the leishmanial parasite, and inhibition of TryR could potentially disrupt the redox balance of the parasite leading to the parasite death [22]. The synthesized tetrazole derivative **(4)** was computationally docked into the pocket of trypanothione reductase (TryR)

https://doi.org/10.1016/j.heliyon.2018.e00792

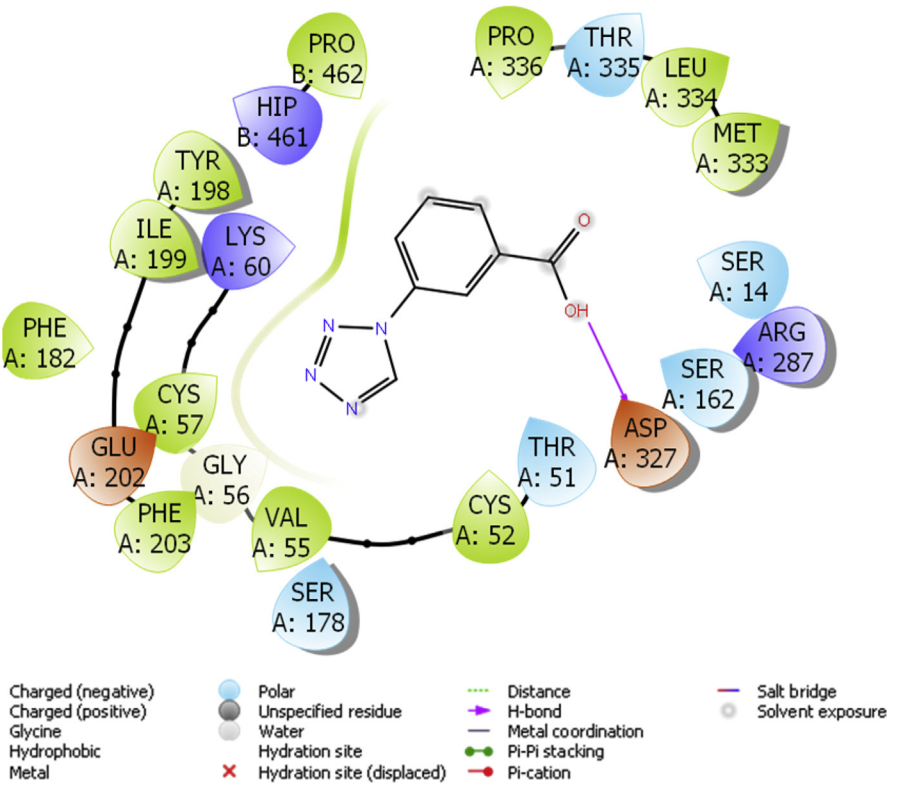

Fig. 7. Binding mode of tetrazole derivative **(2)** inside the active site of TryR in two dimensional space.

enzyme, required for redox balance of the parasite. Glide docking module, offered by Schrodinger program [23] was used to carry out the molecular docking of synthesized molecule with the protein. The synthesized tetrazole derivative **(4)** under analysis showed satisfactory docking with acceptable statistics inside the active site of TryR. The enzyme (TryR) is a dimer and chain A was selected for the docking studies. Docking analysis of the ligand with TryR protein enabled us to identify specific residues which constructed the active site. Following residues are found surrounding docked poses of the ligand, Lue10, Gly11, Ala12Gly13, Ser14, Gly15, Gly16, Val34, Asp35, Val36, Ala46, Ala47, Gly49, Gly50, Thr51, Cys52, Gly125, Phe126, Gl127, Ala159, Thr160, Ser162, Arg290, Ala293, Leu294, Ile325, Gly326, Asp327, Val328, Ala338, Met333, Leu334, Thr335, and Ala338. These residues can possibly play important functional roles in enzyme activities. Therefore, interaction of the ligand with these residues could influence the structure of the active site, consequently leading to the inhibition of the activities of the enzyme TryR.

The detailed analysis of the binding mode of the ligand with TryR receptor revealed that the ligand stabilized itself inside the active site gorge by copious interactions with the atoms of the key residues of receptor TryR. Tetrazole ring of the ligand formed π-π stacking with phenyl ring of Phe182 (Fig. 8), similarly, phenyl ring of ligand also played important role in binding the ligand inside the pocket through

https://doi.org/10.1016/j.heliyon.2018.e00792

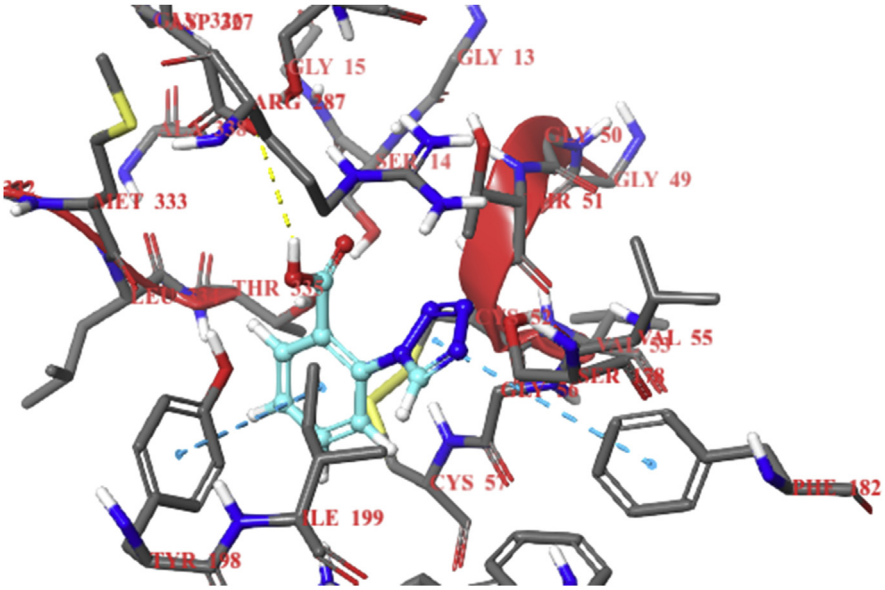

Fig. 8. The docking pose of synthesized tetrazole derivative **(4)** inside the active site of TryR presented in three-dimensional space. The ligand is shown in ball and stick mode, carbon atoms are shown in cyan color and non-carbon atoms are shown in elemental color. Amino acid residues are shown in stick mode and elemental color. π-π Stacking of the aromatic rings of ligand with those of amino acids are shown in cyan colored dashed lines while hydrogen bonding of ligand atom with the residue atom is shown in yellow colored dashed lines.

a π-π stacking with the phenyl ring of Try198 as shown in Figs. 8 and 9. In addition to that, oxygen atom of the ligand formed determinant hydrogen bonding such as O—H…O with the Ala338 inside the pocket of TryR (Fig. 8). Moreover, compound was found to interact favorably with protein with a very good docking and Glide score of −6.217 kcal/mol.

2.7. Results and discussion of docking computation of (6)

A theoretical docking study was conducted in order to investigate the potential anti-leishmanial properties of the tetrazole derivative **(6)** against TryR. Trypanothione reductase (TryR) is involved in the redox metabolism of the leishmanial parasite, and inhibition of TryR could potentially disrupt the redox balance of the parasite leading to death of the parasite [22]. The tetrazole derivative **(6)** was computationally docked into the pocket of trypanothione reductase (TryR) enzyme, required for redox balance of the parasite. Glide docking module, offered by Schrodinger program [23] was used to carry out the molecular docking of synthesized molecule on protein. The compound under analysis showed acceptable docking with satisfactory statistics inside the active site of TryR. The enzyme (TryR) is a dimer consisting of two active sites and the active site from chain A was selected for the docking studies. Docking analysis of the ligand with Try protein enabled us to identify specific residues which constructed the active site. Following residues, Lue10, Gly11,

https://doi.org/10.1016/j.heliyon.2018.e00792

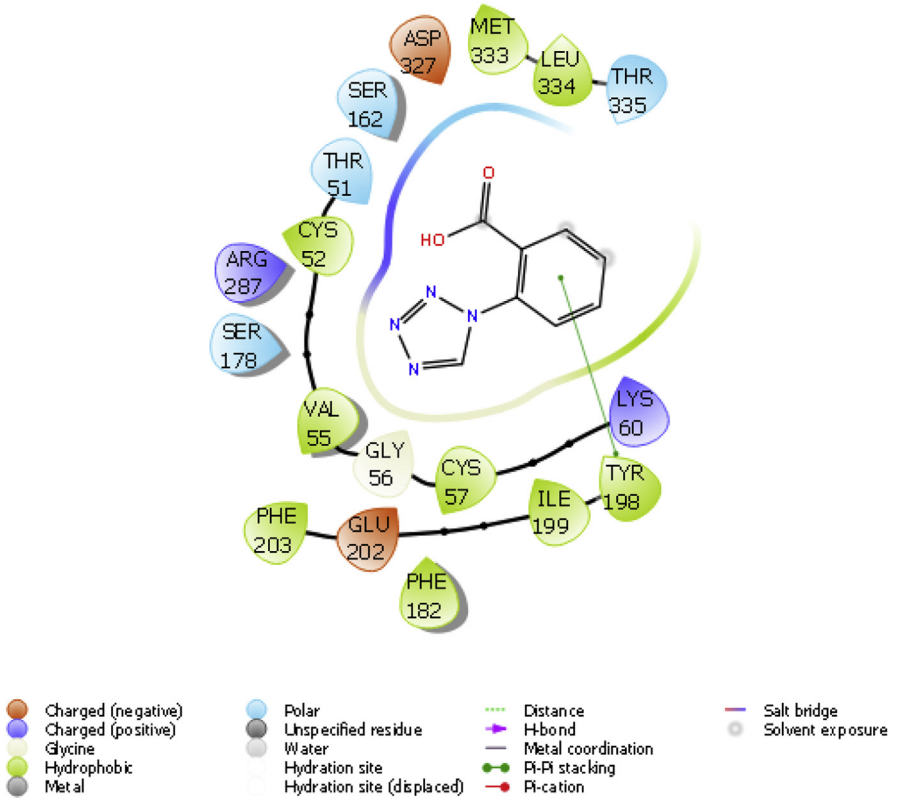

Fig. 9. Binding mode of the synthesized tetrazole derivative **(4)** inside the active site of TryR in two dimensional space.

Ala12 Gly13, Ser14, Gly15, Gly16, Val34, Asp35, Val36, Ala46, Ala47, Gly49, Gly50, Thr51, Cys52, Gly125, Phe126, Gl127, Ala159, Thr160, Ser162, Arg290, Ala293, Leu294, Ile325, Gly326, Asp327, Val328, Ala338, Met333, Leu334, Thr335, and Ala338 are found surrounding docked poses of the ligand. These residues can play important functional roles in enzyme activities. Therefore, interaction of the ligand with these residues could possibly disrupt the function of the enzyme, consequently leading to inhibition of the activities of the enzyme TryR.

The comprehensive exploration of the binding mode of the ligand with TryR receptor revealed that the ligand stabilized itself inside the active site gorge by copious interactions with the atoms of the key amino acid residues of the receptor TryR. Ligand stabilized itself through multiple hydrogen bonding in addition to a stacking as shown in Figs. 10 and 11. Two nitrogen atoms of the tetrazole ring of the ligand formed hydrogen bonding with the Ser14 and Cys52, such as N…N—H (Fig. 10). Both the oxygen atoms of the ligand also played a significant role in binding the ligand inside the active site by establishing the hydrogen bonding with Thr51 and Val53. Moreover, compound interacted favorably with TryR protein with a considerable docking and Glide score of −5.955 kcal/mol.

https://doi.org/10.1016/j.heliyon.2018.e00792

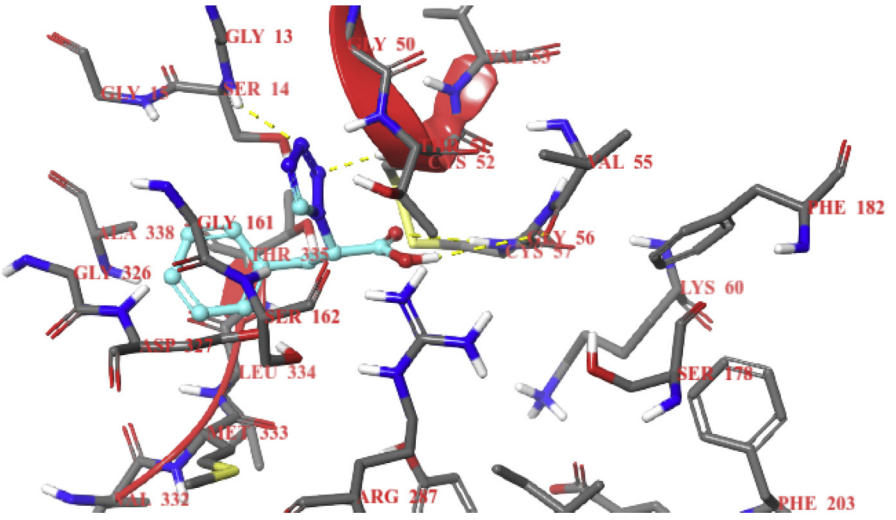

Fig. 10. Binding mode of the tetrazole derivative **(6)** inside the active site of TryR. Docking poses of compound in tri-dimensional space. Ligand is shown in ball and stick mode in elemental and cyan color. Key segments of the amino acid residues are shown in stick mode with hydrogen bonds between the ligand and the amino acids drawn as dashed yellow lines.

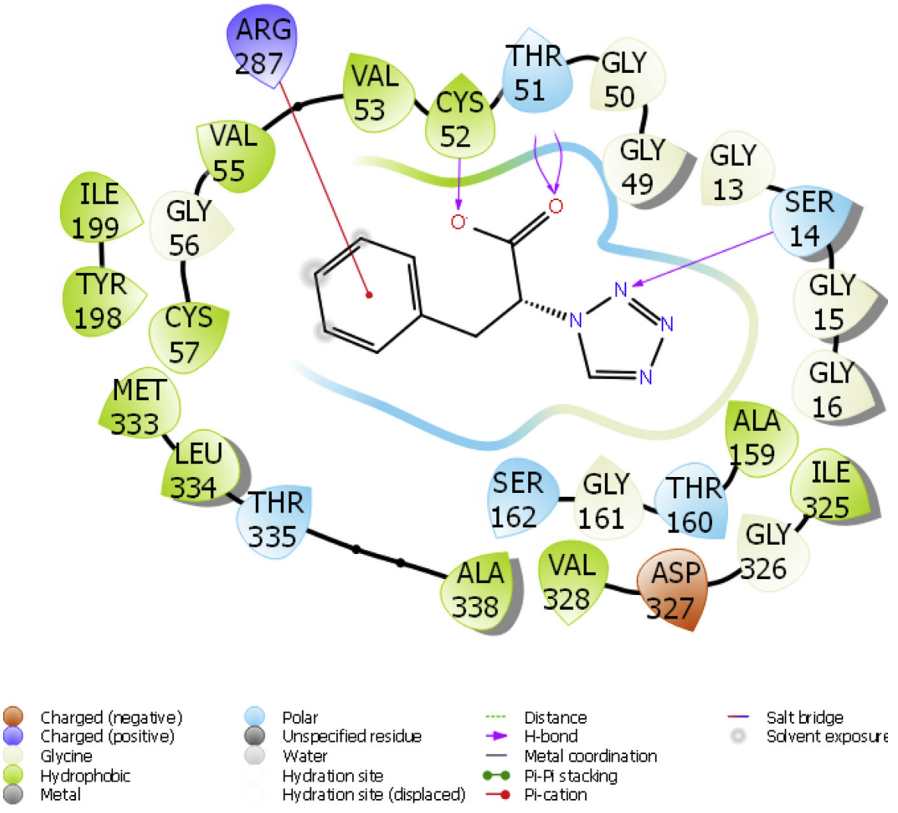

Fig. 11. Binding mode of the tetrazole derivative **(6)** inside the active site of TryR in two dimensional space.

https://doi.org/10.1016/j.heliyon.2018.e00792

2.8. Structure activity relationship (SAR)

The efficient delocalization of negative charge over tetrazole rings lead to a favorable interactions thereby help to increase the efficacy of tetrazole based drugs. Based on these observations, the present research work presents the cytotoxicity and antileishmanial evaluation of tetrazole derivatives **(2, 4, 6)**. The tested tetrazole derivatives **(2, 4, 6)**, were found to be biocompatible with respect to their cytotoxicity evaluation on human red blood cells (52.89, 17.28, 49.33 μg/ml). Among the tested tetrazole derivatives **(2, 4, 6)**, the derivative **(2)** presented interesting antileishmanial activity against the promastigotes stage of *Leishmania tropica* ($IC_{50} = 0.166$ μg/ml) as given above in Table 1. The tested tetrazole derivatives **(2, 4)** are isomeric in nature and differ only in the position of COOH group on the phenyl ring. In **(2)** when the hydrophilic COOH is at *meta* position is found to be most potent while compound **(4)** having the same group at *ortho* position is shows intermediate activities in both activities. On the other hand, in **(6)** in which the COOH is not a part of aromatic ring at all, rather attached to an aliphatic carbon is least active. This has been explained by docking studies.

The cytotoxicity (LD_{50}) and the *antileishmanial activity* (IC_{50}) of the tested derivatives were compared to assess the corresponding selectivity index ($SI = LD_{50}/IC_{50}$). Among the tested derivatives, the tetrazole derivative **(2)** presented greater selectivity index for promastigotes stage of *Leishmania tropica* and least for tetrazole derivatives **(4, 6)**. Structure activity relationship suggests the effect of the electron withdrawing carboxyl group on the tetrazole derivatives. The carboxyl group at *para* position of tetrazole derivative **(2)** enhances the antileishmanial activity against promastigotes of *Leishmania* tropica.

3. Experimental

3.1. Materials and method

All of the reagents and solvents required were purchased from Sigma-Aldrich and were used without any further purification. Glassware for performing chemical reaction performed were dried in an oven at 140 °C for minimum of 6 hours prior to use. ^{1}H and ^{13}C nuclear magnetic resonance (NMR) spectra were recorded using DMSO-d_6 as a solvent on a Bruker spectrometer at 300 and 75 MHz, respectively. DMSO-d_6 was used as solvent and TMS was used as an internal reference. Chemical shifts are given in δ scale (ppm). FT-IR spectra were recorded on the Vertex 70 Bruker apparatus. Elemental analysis (CHN) was performed to find out the percentage of the each element present in the synthesized compound. The progress of the reactions was checked by thin-layer chromatography (TLC) on 2.0 cm × 5.0 cm aluminium sheets precoated with silica gel 60F254 with a layer thickness of 0.25 mm (Merck).

https://doi.org/10.1016/j.heliyon.2018.e00792

Crystals of the synthesized compound were grown by slow evaporation of ethanol at room temperature.

3.2. Procedure for the synthesis of tetrazole derivatives (2, 4, 6)

The tetrazole derivatives **(2, 4, 6)** were synthesized according to the literature reported method but with minor modifications. In a typical experiment, glacial acetic acid (15 ml) was added to a suspension of amino benzoic acids (10 mmol) and sodium azide (10 mmol) in triethyl orthoformate (20 mmol) with constant stirring at 400 rpm. The reaction mixture was than stirred at 150 °C on an oil bath for almost 10 hours. Thin layer chromatography was constantly used to monitor the progress of the reaction. Upon completion of the reaction, a mixture of concentrated Hydrochloric acid (37%) and Water (25 ml) was poured in the flask till solid precipitates were formed. The solid precipitates formed, were separated by filtration and dried in oven at 50 °C. The synthesized tetrazole derivatives **(2, 4, 6)** were obtained in good to excellent yields (75%, 63%, 84%) respectively. The oven dried solid precipitates of the tetrazole derivatives **(2, 4, 6)** were efficiently purified by recrystallization technique.

3.3. Purification of the tetrazole derivatives (2, 4, 6)

Once the tetrazole derivatives **(2, 4, 6)** were successfully synthesized, the compounds **(2, 4, 6)** were purified using column chromatography (30% hexane: ethyl acetate) which yield the purified compounds as solid precipitates. The tetrazole derivatives **(2, 4, 6)** were further purified by recrystallization method from ethanol. Briefly, the synthesized tetrazole derivatives obtained were dissolved in ethanol and supersaturated solutions of **(2, 4, 6)** were prepared at 50 °C. The prepared supersaturated solution of **(2, 4, 6)** were placed in glass vials covered with a lid to evaporate ethanol slowly from the solution at room temperature. Crystals of **(2, 4, 6)** appeared gradually as the evaporation of ethanol started at room temperature [19]. The crystals obtained were separated from the mixture, dried and were analysed using single crystal XRD to confirm the structure of tetrazole derivatives **(2, 4, 6)**. The characterization data of the tetrazole derivatives including ^{1}H NMR, ^{13}CNMR, CHN analysis is provided below for each of the synthesized tetrazole derivatives **(2, 4, 6)**.

3.4. Characterization data of the synthesized tetrazole derivatives (2, 4, 6)

3.4.1. 3-(1H-tetrazol-1-yl) benzoic acid (2)

White powder; Yield 75%; Mol. wt: 190.1; ^{1}H NMR (DMSO-d_6), 11.28 (s, 1H, OH), 8.58 (s, 1H, CH), 8.19 (s, 1H), 8.09 (d, 1H), 7.8 (d, 1H), 7.14 (m, 1H); ^{13}C NMR

https://doi.org/10.1016/j.heliyon.2018.e00792

(DMSO-d_6), 168.40 (C═O), 140.1 (CH-Tetrazole ring), 134.25 (C_4), 130.45(C_6), 130.45(C_1), 128.34 (C_5), 120.4(C_3), 118.30(C_2); Anal. Cald. For $C_8H_6N_4O_2$: C, 50.53; H, 3.28; N, 29.40; O, 16.77.

3.4.2. 2-(1H-tetrazol-1-yl) benzoic acid (4)

Yellow powder; Yield 63%; Mol. wt: 190.1; ^{1}H NMR (DMSO-d_6), 11.01 (s, 1H, OH), 8.9 (s, 1H, CH), 8.0 (d, 1H), 7.60 (m, 1H), 7.4 (d, 1H), 7.34 (m, 1H); ^{13}C NMR (DMSO-d_6), 169.40 (C═O), 140.41 (CH-Tetrazole ring), 134.1 (C_4), 132.3(C_6), 130.45(C_1), 129.4 (C_5), 128.4(C_3), 127.30(C_2); Anal. Cald. For $C_8H_6N_4O_2$: C, 50.43; H, 3.10; N, 29.45; O, 17.1.

3.4.3. 3-phenyl-2-(1H-tetrazol-1-yl)propanoic acid (6)

White powder; Yield 84%; Mol. wt: 218.2; ^{1}H NMR (DMSO-d_6), 11.0 (s, 1H, OH), 8.78 (s, 1H, CH), 7.30 (d, 2H), 7.10 (m, 2H), 7.8 (d, 1H); ^{13}C NMR (DMSO-d_6), 171.10 (C═O), 142.3 (CH-Tetrazole ring), 134.25 (C_4), 128.5(C_2), 127.4(C_3), 126.4 (C_4), 64.1 (1H), 32.2 (2H); Anal. Cald. For $C_{10}H_{10}N_4O_2$: C, 55.14; H, 4.56; N, 25.74; O, 14.66.

3.5. Crystal structure determination of (2) · H_2O

$C_8H_6N_4O_2 \cdot H_2O$, $M_r = 208.2$, colorless crystal, size 0.46 × 0.08 × 0.06 mm^3, monoclinic space group ***P 2$_1$/n*** with $Z = 4$, a = 12.435(2), b = 3.6715(6), c = 20.015(3) Å, β = 102.511(4)°, V = 892.1(3) Å^3; $D_c = 1.550$ Mg/m^3, μ = 0.122 mm^{-1}, F(000) = 432. The intensity data were recorded using a Bruker SMART CCD area-detector diffractometer [25] with graphite monochromated MoK_α radiation ($\lambda = 0.71073$ Å) at T = 130(2) K. 7739 reflections collected 1.8 >Θ> 27.9°; 2109 independent reflections $I > 2\sigma(I)$, $R_{int} = 0.033$. Structure solution by direct methods [26], full-matrix least squares refinement [26] based on F^2 and 145 parameters. The compound crystallizes with one water solvent molecule per asymmetric unit. All but H-atoms were refined anisotropically, hydrogen atoms were clearly located from difference Fourier maps and then refined at idealized positions riding on the carbon or oxygen atoms with isotropic displacement parameters $U_{iso}(H) = 1.2U_{eq}(C)$ and C-H 0.95 Å, $U_{iso}(H) = 1.5U_{eq}(O)$ and O-H 0.84 Å. Water hydrogen atoms were refined freely. Refinement converged at $R1 = 0.039$ [$I > 2\sigma(I)$], w$R2 = 0.107$ [*all data*] and S = 1.04; min./max. ΔF −0.21/0.35 e/Å^3. Crystallographic data for the structure reported in this paper have been deposited with the Cambridge Crystallographic Data Centre as supplementary publication no. CCDC-1571577. Copies of available material can be obtained free of charge via www.ccdc.cam.ac.uk.

https://doi.org/10.1016/j.heliyon.2018.e00792

3.6. Biological activities

3.6.1. Cytotoxic activity

Cytotoxicity was performed using a method of Nadhman et al., 2015 but with minor modifications [27]. Briefly, 180 μL fresh human red blood cells were washed three times at 3000 rpm with phosphate buffer solution (PBS). The suspensions of the blood cell were incubated with 20 μL of compound with different concentrations (1000, 500, and 250 μg) at 37 °C for 3 hours. After incubation, the suspended cells were centrifuged at 6000 rpm for 10 minutes. Using Uv-visible spectrophotometry (T80, pg instruments), the released hemoglobin was assessed at 576 nm by taking the supernatant. Triton X-100 (0.1%) was taken as positive control and the red blood cell suspension in PBS without compound was used as a negative control. Percent hemolysis was calculated by this formula:

$$\%\text{Hemolysis} = \frac{(\text{OD at } 576\,\text{nm in the compound solution} - \text{OD at } 576\,\text{nm in PBS})}{(\text{OD at } 576\,\text{nm in } 0.1\%\ \text{Triton X} - 100 - \text{OD at } 576\,\text{nm in PBS})} \times 100$$

3.6.2. Antileishmanial activity

For anti-leishmanial assay, stock solution of tetrazole derivatives **(2, 4, 6)** were prepared by dissolving 1 mg/1 ml of DMSO. *Leishmania tropica* KWH23 Promastigotes were grown in the M199 (Medium 199). Media was prepared by modified method of Nadhman et al., 2014 [28]. Briefly, cells were cultured in M199, streptomycin, 25 mM HEPES Buffer(4-(2-hydroxyethyl)-1-piper-azi-neethanesulfonic acid) supplemented with 10% heat inactivated FBS with pH 7.2 and maintained at a temperature of 24 °C. Medium 199 containing culture of Promastigotes were suspended in the wells of a 96-well microtiter plates. After counting cells on Neubauer chamber, Promastigotes were suspended to yield 2×10^6 cell/ml in each well. Afterwards, as a reference drug compound was treated serially in each well of the plate and 2 wells were left for positive and negative control. DMSO was taken as negative control and successively diluted in the M199 medium. Glucantime was used as positive control and then overnight incubated in the dark at 25 °C for 72 hours. The number of viable cells was counted on the Neubauer chamber under microscope (Micros, AUSTRIA). All the in-vitro reactions were carried out in triplicate and results were expressed as a % inhibition in parasite numbers. The drug concentration required for 50% inhibition. IC_{50} values of the tetrazole derivatives **(2, 4, 6)**, showing anti-leishmanial activity, were determined by SPSS22 software.

https://doi.org/10.1016/j.heliyon.2018.e00792

3.7. Molecular docking method

The crystal structure of the protein, was obtained from RCSB (PDB ID: 2JK6) [29] and was used for modeling purposes. ProteinPrep wizard of the Schrodinger program [30] was used to prepare protein for docking studies. Since the receptor contains cognate ligand therefore a grid was generated for docking purposes by creating a box centroid at the cognate ligands of the TRyR. The ligand was drawn in Maestro workspace using the builder module [31], hydrogens were added and ligand was saved in three dimensional geometry for further use. The ligand was prepared using the Ligprep module offered by Schrodinger program [32], and was used for further molecular docking studies. The Glide standard precision (Glide-SP) module was used for docking simulations [24].

4. Conclusions

The present paper describes in detail the synthesis, molecular structure and bio-assay of tetrazole derivatives **(2, 4, 6)**. The substituted tetrazole derivatives **(2, 4, 6)** were synthesized in good yields and their crystal structures were determined using single crystal X-ray diffraction analysis. The crystal structure diversities of the tetrazoles **(2, 4, 6)** and various interactions responsible for their crystal stability are depicted in detail. In addition, *in vitro* cytotoxic and antileishmanial activity of the tetrazole derivatives **(2, 4, 6)** was also evaluated. The better *in vitro* biocompatibility and antileishmanial activity of the tetrazole derivatives **(2, 4, 6)** could be a better choice for further evaluation as therapeutic agents against leishmaniasis upon comparison with the standard drug (Glucantime). Molecular docking studies of the compounds with the TryR macromolecule could provide the first hand evidence for binding of compounds in active site of TryR. Thus, the synthesized tetrazole derivatives **(2, 4, 6)** can be possible hit candidate which can be tested further against amastigote stage of parasite and then in an animal model of leishmaniasis.

Declarations

Author contribution statement

Hamid Aziz: Performed the experiments; Analyzed and interpreted the data; Wrote the paper.

Aamer Saeed: Conceived and designed the experiments; Wrote the paper.

Farukh Jabeen, Noor ud Din: Analyzed and interpreted the data.

Ulrich Flörke: Performed the experiments.

https://doi.org/10.1016/j.heliyon.2018.e00792

Funding statement

Hamid Aziz was supported by the Indigenous PhD Fellowships for 5000 Scholars, Phase-II, Batch-I from the Higher Education Commission of Pakistan.

Competing interest statement

The authors declare no conflict of interest.

Additional information

No additional information is available for this paper.

References

[1] D.J. Brown, A.R. Katritzky, C.W. Rees, in: A.R. Katrizky (Ed.), Comprehensive Heterocyclic Chemistry, vol. 2, 1984, pp. 150−189.

[2] H.B. Jonassen, et al., Platinum-and palladium-tetrazole complexes, Inorg. Chem. 9 (1970) 2678−2681.

[3] Z.P. Demko, K.B. Sharpless, Preparation of 5-substituted 1 H-tetrazoles from nitriles in water, J. Org. Chem. 66 (2001) 7945−7950.

[4] T. Zhao, Novel Application of Tetrazoles Derived from the TMSN3-Ugi Reaction, Rijksuniversiteit Groningen, 2016.

[5] S. Berghmans, et al., Zebrafish offer the potential for a primary screen to identify a wide variety of potential anticonvulsants, Epilepsy Res. 75 (2007) 18−28.

[6] J.H. Toney, et al., Antibiotic sensitization using biphenyl tetrazoles as potent inhibitors of Bacteroides fragilis metallo-β-lactamase, Chem. Biol. 5 (1998) 185−196.

[7] C.X. Wei, M. Bian, G.H. Gong, Tetrazolium compounds: synthesis and applications in medicine, Molecules 20 (2015) 5528−5553.

[8] M. Alam, et al., Computational and anti-tumor studies of 7a-Aza-B-homostigmast-5-eno [7a, 7-d] tetrazole-3β-yl chloride, J. Mol. Struct. 1108 (2016) 411−426.

[9] Y. Tamura, et al., Highly selective and orally active inhibitors of type IV collagenase (MMP-9 and MMP-2): N-sulfonylamino acid derivatives, J. Med. Chem. 41 (1998) 640−649.

https://doi.org/10.1016/j.heliyon.2018.e00792

[10] V.A. Ostrovskii, et al., Energetic 1, 2, 4-triazoles and tetrazoles: synthesis, structure and properties, ChemInform 31 (2000) 50.

[11] M. Hiskey, et al., Progress in high-nitrogen chemistry in explosives, propellants and pyrotechnics, in: Proc Int Pyrotech Semin, 2000.

[12] C.P. Lawler, et al., Interactions of the novel antipsychotic aripiprazole (OPC-14597) with dopamine and serotonin receptor subtypes, Neuropsychopharmacology 20 (1999) 612−627.

[13] K.D. Burris, et al., Aripiprazole, a novel antipsychotic, is a high-affinity partial agonist at human dopamine D2 receptors, J. Pharmacol. Exp. Therapeut. 302 (2002) 381−389.

[14] N. Mekni, A. Baklouti, Synthesis of new 1-substituted 4-perfluoroalkyl tetrazol-5-ones, J. Fluorine Chem. 129 (2008) 1073−1075.

[15] A.L. Jackman, et al., Cellular pharmacology and in vivo activity of a new anticancer agent, ZD9331: a water-soluble, nonpolyglutamatable, quinazoline-based inhibitor of thymidylate synthase, Clin. Canc. Res. 6 (1997) 911−921.

[16] J.V. Faria, et al., Synthesis and activity of novel tetrazole compounds and their pyrazole-4-carbonitrile precursors against Leishmania spp, Bioorg. Med. Chem. Lett 23 (2013) 6310−6312.

[17] V. dos Santos Faiões, M.S. dos Santos, A.M.R. Bernardino, E.F. Cunha-Junior, M.M. do Canto Cavalheiro, E.C. Torres-Santos, The new pyrazolyltetrazole derivative MSN20 is effective via oral delivery against cutaneous leishmaniasis, antimicrobia, Agents Chemother. 58 (2014) 6290−6293.

[18] V. dos Santos Faiões, L.L. Leon, M.M. Canto-Cavalheiro, E.C. Torres-Santos, A.M. Bernardino, P.F. Vegi, M.S. dos Santos, Effectiveness of novel 5-(5-amino-1-aryl-1H-pyrazol-4-yl)-1H-tetrazole derivatives against promastigotes and amastigotes of leishmania amazonensis, Chem. Biol. Drug Des. 83 (2014) 272−277.

[19] S. Voitekhovich, et al., Synthesis of new functionally substituted 1-R-tetrazoles and their 5-amino derivatives, Chem. Heterocycl. Comp. 41 (2005) 999−1004.

[20] Lyakhov, S. Alexender, et al., 2-(1H-Tetrazol-1-yl) benzoic acid, Acta Crystallogr. Sect. C Cryst. Struct. Commun. 57 (12) (2001) 1436−1437.

[21] Jie Xia, Hong Zhao, 3-Phenyl-2-(1H-tetrazol-1-yl) propanoic acid monohydrate, Acta Crystallogr. E: Struct. Rep. 66 (10) (2010) 2690.

https://doi.org/10.1016/j.heliyon.2018.e00792

[22] R. Mushtaq, et al., A structural investigation of heteroleptic pentavalent antimonials and their leishmanicidal activity, Appl. Organomet. Chem. 30 (2016) 465−472.

[23] R.K. Gundampati, M.W. Jagannadham, Molecular Docking Based Inhibition of Rypanothione Reductase Activity by Taxifolin Novel Target for Antileishmanial Activity, 2012.

[24] Schrödinger Release 2017-1: Schrödinger Suite 2017-1. Ligand Docking Protocol; Glide, Schrödinger, LLC, New York, NY, 2017.

[25] Bruker AXS Inc, SMART (Version 5.63), SAINT, Bruker AXS Inc., Madison, WI, USA, 2002, Version 6.02.

[26] G.M. Sheldrick, A short history of SHELX, Acta Crystallogr. A 64 (2008) 112−122.

[27] A. Nadhman, et al., Visible-light-responsive ZnCuO nanoparticles: benign photodynamic killers of infectious protozoans, Int. J. Nanomed. 10 (2015) 6891.

[28] A. Nadhman, et al., PEGylated silver doped zinc oxide nanoparticles as novel photosensitizers for photodynamic therapy against Leishmania, Free Radic. Biol. Med. 77 (2014) 230−238.

[29] P. Baiocco, G. Colotti, S. Franceschini, A. Ilari, Molecular basis of antimony treatment in leishmaniasis, J. Med. Chem. 52 (2009) 2603−2612.

[30] Schrödinger, L.L.C., 2017-1. Schrödinger Release 2017-1: Protein Preparation Wizard, Schrödinger, LLC, New York, NY, 2017.

[31] Schrödinger, Release, 2017-1, Maestro, Schrödinger, LLC, New York, NY, 2017.

[32] Schrödinger, L.L.C., 2017-1. Schrödinger Release 2016-4: Ligprep, Schrödinger, LLC, New York, NY, 2017.

https://doi.org/10.1016/j.heliyon.2018.e00792